

Geometry in CT Reconstruction

Copyright 2011 Benjamin Kimia

February 22, 2011

Contents

1	Introduction to CT Reconstruction	3
1.1	Linear Attenuation Coefficient	3
1.2	Linear Tomography	5
1.3	Radon Transform	6
1.4	Understanding Back Projection	8
1.5	The Fourier Approach to CT Reconstruction	12
1.6	Filtered Backprojection	12
1.7	Watch out for those singularities: A review of Calculus	17
1.8	The Spatial Domain Approach to CT Reconstruction	18
1.9	Inverse Radon Transform	20
2	Fan Beam Geometry	21
2.1	Radon Transform and Fan Beam Geometry	24
2.2	Radon Inversion Formula for Fan Beam Geometry	26
2.3	Convolution in Fan Beam Geometry	30
3	Flirting with Filtering	32
3.1	Introduction	32
3.2	Filtering	32
3.3	Matched Filtering	36
3.4	Detecting Spots	37
3.4.1	Detecting A Gaussian Spot	37
3.4.2	Detecting A Circular Spot	38
4	Taylor Expansion in the View Space	41
5	Geometric Tomography	41
5.1	Fan Beam Geometry	46

6	Cone Beam Tomography and Volumetric CT	48
6.1	Notation and Definition	50
6.2	Relating Cone Beam and Radon Transform	54
6.3	Reconstruction Algorithms for Cone Beam Helical CT	57
6.4	History of Helical Cone Beam CT Development	63
6.5	Material to be worked into this section	64
6.6	Numerical algorithms for helical cone-beam reconstruction	65
7	Radon's Proof	66
8	To Do	67
A	Integrals Involving Gaussians and Derivatives of Gaussians	71
A.1	Integrals involving a Gaussian and its derivatives	71
A.2	Fourier Transform of the Gaussian	72
A.3	Integrals of the Gabor Filter	73
A.4	74
B	Integrals Involving Characteristic Function of Circular Domains	77
B.1	77
B.2	78
C	Some Standard Fourier Formulas	79
D	A Numerically stable method to find an extremum	80
E	Solving $A \sin \theta + B \cos \theta = C$	81
F	Π-line membership	83
F.1	References not included in the paper yet	88

1 Introduction to CT Reconstruction

The key to CT reconstruction is a characterization of how X-rays are absorbed by material. Since X-rays are electromagnetic waves, we consider how the latter are absorbed as a function of the properties of the material through which the light is traveling, as studied in the field of *optics*. This absorption is governed by the Beer Lambert law, also alternatively known as the Beer's law or the Lambert Beer law or the Beer-Lambert-Bouguer, Figure xx. In short, this law states that the intensity of light passed through a slab of length l drops exponentially with l , *i.e.*,

$$I(l) = I_0 e^{-\alpha l}, \quad (1)$$

where I_0 is the original intensity of the light, etc...

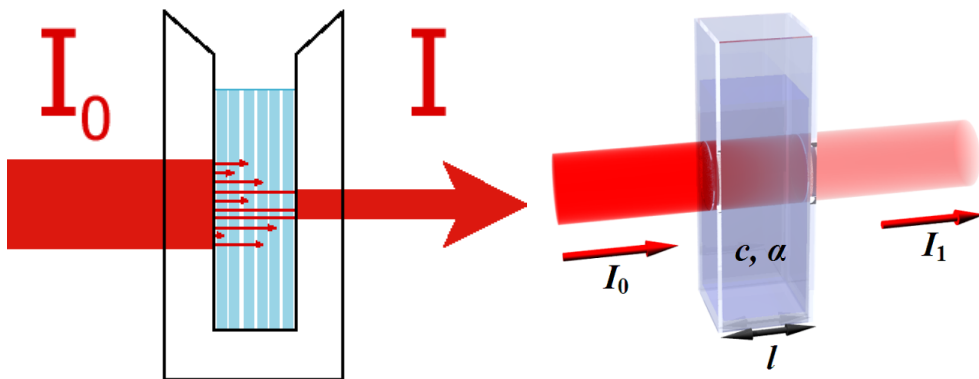


Figure 1: An illustration of the BeerLambert law in optics

1.1 Linear Attenuation Coefficient

Consider an X-ray beam going through some material. The probability that a photon gets removed from a beam (either absorbed or scattered) depends on (i) the energy of the photon, and (ii) the nature of the material through which the beam passes. Define the *linear attenuation coefficient* μ_e^t of tissue t at energy e as

$$\mu_e^t = -\ln(p_e), \quad (2)$$

where p_e is the probability that a photon of energy e transmits through a uniform slab of unit length of tissue t in a direction perpendicular to the face of the slab. For example, the linear attenuation coefficient of water at 73 keV is 0.19 cm^{-1} .

A general model of X-ray absorption is based on an *independence assumption*: The extent of X-ray absorption by the material by any portion of space is independent of that corresponding to the complementary space. This independence is essentially what gives rise to the exponential decay in X-ray intensity. The following discussion is adapted from [11]. Specifically, consider a slab of non-uniform material and denote the linear attenuation coefficient as a function of the coordinate x along the space as $\mu_e(x)$. Let $p_e(x)$ be the probability of absorption in a slab of width dx at x , i.e., the probability that a photon of energy e is transmitted as far as x . Note that $p_e(x)$ is a monotonically decreasing function of x . Now, consider an infinitesimal section dx of the slab from x to $x + dx$. Let $q_e(x, dx)$ denote the probability that a photon of energy e which has reached x will not be transmitted beyond $x + dx$. It is clear, therefore, that the probability of a photon reaching $x + dx$ is the probability of it reaching x and being transmitted through the dx slab:

$$p_e(x + dx) = p_e(x)(1 - q_e(x, dx)),$$

or

$$q_e(x, dx) = -\frac{p_e(x + dx) - p_e(x)}{p_e(x)}.$$

Now let

$$\mu_e(x) = \lim_{dx \rightarrow 0} \frac{q_e(x, dx)}{dx} = -\frac{p_e'(x)}{p_e(x)} = -\frac{d(\ln(p_e(x)))}{dx}.$$

Observe that

$$\int_0^A \mu_e(x) dx = -\int_0^A -\frac{d(\ln(p_e(x)))}{dx} dx = -\ln(p_e(x))|_0^A = -\ln(p_e(A)) + \ln(1) = -\ln(p_e(A)).$$

Now, for a uniform slab of unit length, *i.e.* where $\mu_e(x) = \mu_e$ and $A = 1$, we have

$$\mu_e = \int_0^1 \mu_e(x) dx = -\ln(p_e(1)).$$

Comparing this to Equation(2), it is clear that $\mu_e = \mu_e^t$. Since q_e as a probability is dimensionless, μ_e has dimension of $length^{-1}$ and so does μ_e^t .

In actual practice, since calibration is required to make measurements uniform across detection, the actual linear attenuation coefficient μ_e^t is measured relative to μ_e^c , the linear attenuation coefficient of the calibration material. Define the *relative linear attenuation coefficient* as

$$\mu_e^{t,a} = \mu_e^t - \mu_e^a.$$

Note that line integrals of these quantities are simply related:

$$\begin{aligned}
 \int_0^A \mu_e^{t,a}(x) dx &= \int_0^A (\mu_e^t(x) - \mu_e^a(x)) dx \\
 &= \int_0^A \mu_e^t(x) dx - \int_0^A \mu_e^a(x) dx \\
 &= -\ln(p_e^t(A)) + \ln(p_e^a(A)) \\
 &= -\ln\left(\frac{p_e^t(A)}{p_e^a(A)}\right).
 \end{aligned}$$

The *CT number* is defined as

$$H = 1000 \frac{\mu_e^t - \mu_e^{water}}{\mu_e^{water}}, \quad (3)$$

which is scaled so that the CT number of water is 0 and the CT number of air is -1000. CT numbers are expressed in Hounsfield units¹

Tissue	CT-Number (H)
Lung	-300
Fat	-90
White Matter	30
Gray Matter	40
Muscle	50
Trabecular Bone	300-500
Cortical Bone	600-3,000

1.2 Linear Tomography

Linear Tomography is a technique used to emphasize certain depths in patients before computers could be used to do this. Basically, with the patient on the table, the X-ray source and film were moved in opposite directions, each at a fixed rate. Transaxial Tomography essentially accomplishes the same idea by rotating both the patient and the film at the same speed.

The basic idea is that the images of two points A and B (both at depth h with respect to the source), \overline{A} and \overline{B} , have a distance $|\overline{A} \overline{B}| = \frac{h}{h} |AB|$,

¹[From Wiki] Sir Godfrey Newbold Hounsfield CBE, FRS, (28 August 1919 – 12 August 2004) was an English electrical engineer who shared the 1979 Nobel Prize for Physiology or Medicine with Allan McLeod Cormack for his part in developing the diagnostic technique of X-ray computed tomography (CT).

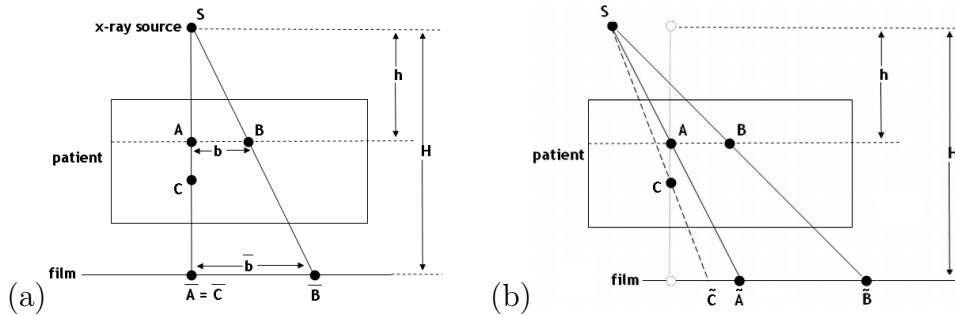


Figure 2: Linear Tomography was used to focus on a plane at a certain depth by moving both the source and the film in a predetermined fashion

regardless of the position of S , as long as the depth h is fixed and correspondance is maintained. Figure(2) shows the process of emphasizing the plane at depth h from the source. Thus, the film and the source can be moved simultaneously so that the image of A on the film in the new position of the film, \tilde{A} , corresponds exactly to \bar{A} . Since $|\tilde{A} \tilde{B}| = |\bar{A} \bar{B}| = \frac{H}{h}|AB|$, all points at the same depth align with their corresponding points. For points at other depths, however, there is no correspondance and each point C contributes to points in an extended range. Thus, the effect of these points is to add more blurring to the film, but at the same time isolating the contribution of points at depth h since they add up in the same spot on the film. Linear and transaxial tomography motivate the idea of backprojection as a way of finding the linear attenuation coefficient at each point. We first develop some formalities.

1.3 Radon Transform

Let $\mu(x, y)$ represent the distribution of the X-ray absorption/attenuation coefficients in Hounsfield units. This is our unknown. We will assume throughout this document that μ is continuous and bounded, and that it vanishes outside the region of interest (scanning area). *The Radon Transform*, R_μ is a map from $\mu(x, y)$ to a 1-D function $\rho_\theta(\xi)$ where θ is the angle along lines of X-ray projection and ξ is the variable orthogonal to these lines (Figure 3), *i.e.*,

$$\begin{aligned}
 \rho_\theta(\xi) &= \int_{-\infty}^{\infty} \mu(x(\xi, \eta), y(\xi, \eta)) d\eta \\
 &= \int_{-\infty}^{\infty} \mu(\xi \cos \theta - \eta \sin \theta, \xi \sin \theta + \eta \cos \theta) d\eta.
 \end{aligned} \tag{4}$$

We also often use $R_\mu(\xi, \theta)$ or $\rho(\xi, \theta)$ to denote the Radon Transform over a range of angles.

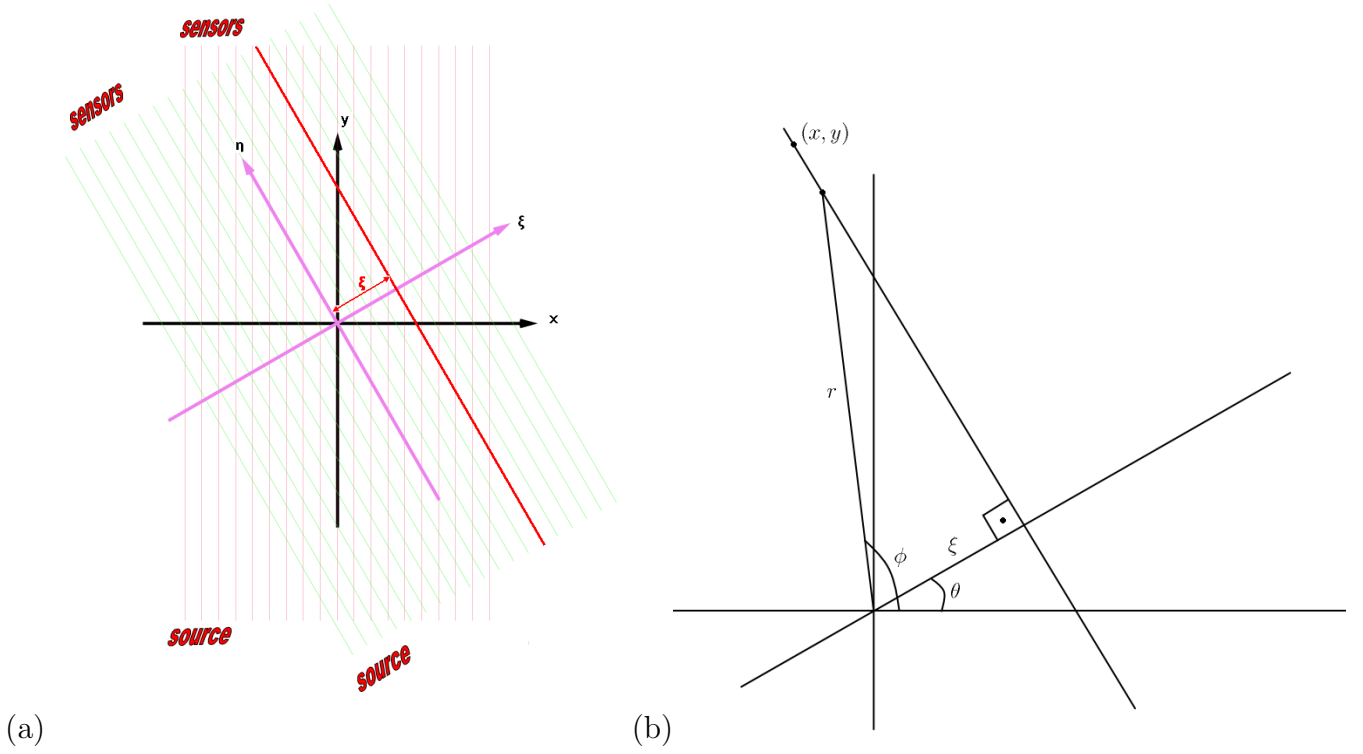


Figure 3: (a) The Radon Transform is the line integral of μ , where each line represents the X-ray that goes from source to sensor. The line can be expressed as $\xi = \xi_0$ in a rotated coordinate system in (b).

Ideally, these measurements need to be made only for $\theta \in [0, \pi)$ since the entire $[0, 2\pi)$ range can be covered using:

$$\rho_{\theta-\pi}(\xi) = \rho_\theta(-\xi). \quad (5)$$

Note that:

$$\begin{bmatrix} x \\ y \end{bmatrix} = \begin{bmatrix} \cos \theta & -\sin \theta \\ \sin \theta & \cos \theta \end{bmatrix} \begin{bmatrix} \xi \\ \eta \end{bmatrix} \text{ and } \begin{bmatrix} \xi \\ \eta \end{bmatrix} = \begin{bmatrix} \cos \theta & \sin \theta \\ -\sin \theta & \cos \theta \end{bmatrix} \begin{bmatrix} x \\ y \end{bmatrix}. \quad (6)$$

The set of measurements, $\rho_\theta(\xi)$ where $\theta \in [0, \pi)$ and $\xi \in (-\infty, \infty)$ represents the *view data* or the *sinogram* in the 2-D space spanned by ξ and θ ,

$$\rho(\xi, \theta) = \rho_\theta(\xi). \quad (7)$$

Our goal is to recover $\mu(x, y)$ from $\rho(\xi, \theta)$.

Remark: The Radon Transform is integration along a line. We can specify a line by its distance ξ from the origin and the angle it makes with the x-axis θ . A point (x, y) is on the line if and only if $(x, y) \cdot (\cos \theta, \sin \theta) = \xi$. Thus in a 2D plane $\delta(x \cos \theta + y \sin \theta - \xi)$ is non-zero only when the point (x, y) is on this line. Thus, we see the Radon Transform.

Alternatively, in polar notation, a point (r, ϕ) is on the line if and only if $(r \cos \phi, r \sin \phi) \cdot (\cos \theta, \sin \theta) = \xi$ which reduces to $r \cos(\phi - \theta) = \xi$. This gives an expression for the Radon Transform in polar notation

$$\rho(\xi, \theta) = \int_0^\pi \int_{-\infty}^\infty \mu(r, \phi) \delta(r \cos(\phi - \theta) - \xi) r dr d\phi$$

also written as

$$\rho(\xi, \theta) = \int_{-\infty}^\infty \int_{-\infty}^\infty \mu(x, y) \delta(x \cos \theta + y \sin \theta - \xi) dx dy.$$

1.4 Understanding Back Projection

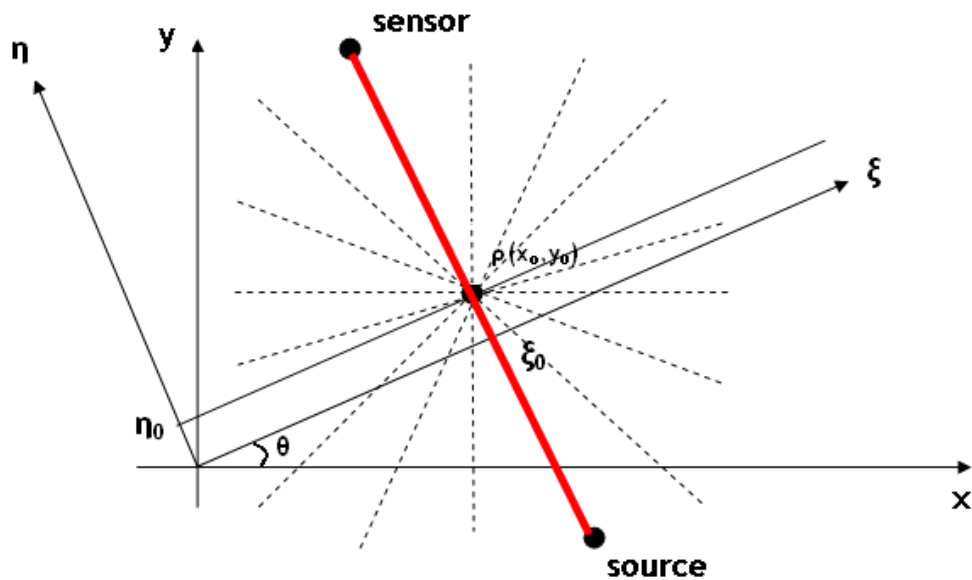


Figure 4: Back projection sums over measurements along rays passing through a fixed point as an estimate of μ there.

The idea of backprojection goes back to *Linear and Transaxial Tomography*. Consider the same idea with a single source and a single sensor rotating around the object around some fixed point $\rho(x_0, y_0)$, Figure(4). The idea is to backproject each view data to all points giving rise to it in an accumulative fashion, *i.e.*, the estimated linear attenuation coefficient at each point in the sum of intensities measured for all rays going through the point. The sensor reading for each ray through ρ , indexed by θ , is obtained from Equation (4)

$$\rho(\xi_0, \theta) = \int_{-\infty}^{\infty} \mu(\xi_0 \cos \theta - \eta \sin \theta, \xi_0 \sin \theta + \eta \cos \theta) d\eta, \quad (8)$$

where $\xi_0 = x_0 \cos \theta + y_0 \sin \theta$. Each ray passes through ρ , but any other point participates in the view data in only one ray. Thus, in the cumulative response, the contribution of all points fades in comparison to that of ρ . The process of accumulating all ray measurements through ρ and using it as an estimate of $\mu(x_0, y_0)$ at ρ is called *backprojection*. Formally,

$$\mu_{BP}(x_0, y_0) = \frac{1}{\pi} \int_0^\pi \rho(\xi_0, \theta) d\theta, \quad \text{where } \xi_0 = x_0 \cos \theta + y_0 \sin \theta. \quad (9)$$

How good an estimate of μ is μ_{BP} ? The following theorem relates the backprojection estimate of μ to μ .

Theorem 1.

$$\mu_{BP}(x, y) = \mu(x, y) * \frac{1}{\pi} \frac{1}{\sqrt{x^2 + y^2}}. \quad (10)$$

Proof. We can relate the two by simplifying Equation (9) using Equation (8):

$$\mu_{BP}(x_0, y_0) = \frac{1}{\pi} \int_0^\pi \left[\int_{-\infty}^{\infty} \mu(\xi_0(\theta) \cos \theta - \eta \sin \theta, \xi_0(\theta) \sin \theta + \eta \cos \theta) d\eta \right] d\theta, \quad (11)$$

where $\xi_0(\theta) = x_0 \cos \theta + y_0 \sin \theta$. We can gain a better insight into this integral by switching to a polar coordinate system centered around (x_0, y_0) ,

$$\begin{cases} x = x_0 + r \cos \phi \\ y = y_0 + r \sin \phi. \end{cases} \quad (12)$$

Now, given (θ, η) in integral (11), these identify (x, y)

$$\begin{cases} x = \xi_0(\theta) \cos \theta - \eta \sin \theta \\ y = \xi_0(\theta) \sin \theta + \eta \cos \theta. \end{cases} \quad (13)$$

Equating (12) and (13) relates (r, ϕ) to (η, θ) :

$$\begin{cases} r \cos \phi = \xi_0(\theta) \cos \theta - \eta \sin \theta - x_0 = (\xi_0(\theta) \cos \theta - \eta \sin \theta) - (\xi_0(\theta) \cos \theta - \eta_0(\theta) \sin \theta) \\ r \sin \phi = \xi_0(\theta) \sin \theta + \eta \cos \theta - y_0 = (\xi_0(\theta) \sin \theta + \eta \cos \theta) - (\xi_0(\theta) \sin \theta + \eta_0(\theta) \cos \theta) \end{cases}$$

or,

$$\begin{cases} r \cos \phi = -(\eta - \eta_0(\theta)) \sin \theta \\ r \sin \phi = (\eta - \eta_0(\theta)) \cos \theta \end{cases}$$

where

$$\begin{cases} \xi_0(\theta) = x_0 \cos \theta + y_0 \sin \theta \\ \eta_0(\theta) = -x_0 \sin \theta + y_0 \cos \theta. \end{cases}$$

When $\eta < \eta_0(\theta)$, we have

$$\begin{cases} r = -(\eta - \eta_0(\theta)) \\ \phi = \theta - \frac{\pi}{2} \end{cases}$$

or, solving for (η, θ)

$$\begin{cases} \eta = -r - x_0 \cos \phi - y_0 \sin \phi \\ \theta = \phi + \pi/2. \end{cases}$$

When $\eta > \eta_0(\theta)$, we have

$$\begin{cases} r = \eta - \eta_0(\theta) \\ \phi = \theta + \frac{\pi}{2} \end{cases}$$

or, solving for (η, θ)

$$\begin{cases} \eta = r + x_0 \cos \phi + y_0 \sin \phi \\ \theta = \phi - \pi/2. \end{cases}$$

In rewriting (9) in terms of r and ϕ , we will also need an expression for $\xi_0(\theta)$.

When $\eta < \eta_0(\theta)$

$$\begin{aligned} \xi_0(\theta) &= x_0 \cos\left(\phi + \frac{\pi}{2}\right) + y_0 \sin\left(\phi + \frac{\pi}{2}\right) \\ &= -x_0 \sin \phi + y_0 \cos \phi. \end{aligned}$$

and when $\eta > \eta_0(\theta)$

$$\begin{aligned}\xi_0(\theta) &= x_0 \cos(\phi - \frac{\pi}{2}) + y_0 \sin(\phi - \frac{\pi}{2}) \\ &= x_0 \sin \phi - y_0 \cos \phi.\end{aligned}$$

We can now rewrite μ_{BP} in (9) as

$$\begin{aligned}\mu_{BP}(x_0, y_0) &= \frac{1}{\pi} \int_0^\pi \int_{-\infty}^{\eta_0(\theta)} \mu(\xi_0(\theta) \cos \theta - \eta \sin \theta, \xi_0(\theta) \sin \theta + \eta \cos \theta) d\eta d\theta \\ &+ \frac{1}{\pi} \int_0^\pi \int_{\eta_0(\theta)}^\infty \mu(\xi_0(\theta) \cos \theta - \eta \sin \theta, \xi_0(\theta) \sin \theta + \eta \cos \theta) d\eta d\theta \\ &= \frac{1}{\pi} \int_{-\frac{\pi}{2}}^{\frac{\pi}{2}} \int_{-\infty}^0 \mu((-x_0 \sin \phi + y_0 \cos \phi)(-\sin \phi) - (-r - x_0 \cos \phi - y_0 \sin \phi)(\cos \phi), \\ &\quad (-x_0 \sin \phi + y_0 \cos \phi)(\cos \phi) + (-r - x_0 \cos \phi - y_0 \sin \phi)(-\sin \phi)) dr d\phi \\ &+ \frac{1}{\pi} \int_{\frac{\pi}{2}}^{\frac{3\pi}{2}} \int_0^\infty \mu((x_0 \sin \phi - y_0 \cos \phi)(\sin \phi) - (r + x_0 \cos \phi + y_0 \sin \phi)(-\cos \phi), \\ &\quad (x_0 \sin \phi - y_0 \cos \phi)(-\cos \phi) + (r + x_0 \cos \phi + y_0 \sin \phi)(\sin \phi)) dr d\phi \\ &= \frac{1}{\pi} \int_{-\frac{\pi}{2}}^{\frac{\pi}{2}} \int_0^\infty \mu((x_0 \sin \phi - y_0 \cos \phi) \sin \phi + (x_0 \cos \phi + y_0 \sin \phi) \cos \phi + r \cos \phi, \\ &\quad (-x_0 \sin \phi + y_0 \cos \phi) \cos \phi + (x_0 \cos \phi + y_0 \sin \phi) \sin \phi + r \sin \phi) dr d\phi \\ &+ \frac{1}{\pi} \int_{\frac{\pi}{2}}^{\frac{3\pi}{2}} \int_0^\infty \mu((x_0 \sin \phi - y_0 \cos \phi) \sin \phi + (x_0 \cos \phi + y_0 \sin \phi) \cos \phi + r \cos \phi, \\ &\quad (-x_0 \sin \phi + y_0 \cos \phi) \cos \phi + (x_0 \cos \phi + y_0 \sin \phi) \sin \phi + r \sin \phi) dr d\phi \\ &= \frac{1}{\pi} \int_0^{2\pi} \int_0^\infty \mu(x_0 + r \cos \phi, y_0 + r \sin \phi) dr d\phi.\end{aligned}$$

We are now in a position to interpret this as an area integral, *i.e.*

$$\begin{aligned}\mu_{BP}(x_0, y_0) &= \frac{1}{\pi} \int_0^{2\pi} \int_0^\infty \left[\frac{\mu(x_0 + r \cos \phi, y_0 + r \sin \phi)}{r} \right] r dr d\phi \\ &= \frac{1}{\pi} \int_{-\infty}^\infty \int_{-\infty}^\infty \frac{\mu(x, y)}{\sqrt{(x - x_0)^2 + (y - y_0)^2}} dx dy \\ &= \mu(x, y) * \frac{1}{\pi} \frac{1}{\sqrt{x^2 + y^2}} \Big|_{x=x_0, y=y_0},\end{aligned}$$

which is the $\frac{1}{r}$ filter well-known from the Fourier approach to the CT reconstruction. In summary, the back projection process gives a *blurred* estimate of $\mu(x, y)$ with a $\frac{1}{r}$ blurring filter. ■

1.5 The Fourier Approach to CT Reconstruction

In this approach, the CT-reconstruction of $\mu(x, y)$ relies on its Fourier Transform,

$$\bar{\mu}(\omega_x, \omega_y) = \mathcal{F}\{\mu(x, y)\} = \int_{-\infty}^{\infty} \int_{-\infty}^{\infty} \mu(x, y) e^{-i\omega_x x} e^{-i\omega_y y} dx dy.$$

Consider a polar representation of $\bar{\mu}$ in the Fourier domain, *i.e.*, $\bar{\mu}(\omega, \theta)$, where $\omega_x = \omega \cos \theta$ and $\omega_y = \omega \sin \theta$. We have

$$\begin{aligned} \bar{\mu}(\omega, \theta) &= \int_{-\infty}^{\infty} \int_{-\infty}^{\infty} \mu(x, y) e^{-i(\omega \cos \theta)x} e^{-i(\omega \sin \theta)y} dx dy \\ &= \int_{-\infty}^{\infty} \int_{-\infty}^{\infty} \mu(x, y) e^{-i(x \cos \theta + y \sin \theta)\omega} dx dy \\ &= \int_{-\infty}^{\infty} \int_{-\infty}^{\infty} \mu(\xi \cos \theta - \eta \sin \theta, \xi \sin \theta + \eta \cos \theta) e^{-i\xi\omega} d\xi d\eta. \end{aligned}$$

The latter integral can be viewed in the form of a 1-D Fourier Transform where θ is fixed, but ω is varying:

$$\begin{aligned} \bar{\mu}(\omega, \theta) &= \int_{-\infty}^{\infty} \left[\int_{-\infty}^{\infty} \mu(\xi \cos \theta - \eta \sin \theta, \xi \sin \theta + \eta \cos \theta) d\eta \right] e^{-i\xi\omega} d\xi \\ &= \int_{-\infty}^{\infty} \rho(\xi, \theta) e^{-i\xi\omega} d\xi \\ &= \mathcal{F}_{\xi}\{\rho(\xi, \theta)\}(\omega) = \bar{\rho}(\omega, \theta), \end{aligned}$$

where $\bar{\rho}(\omega, \theta)$ is the one dimensional Fourier Transform of $\rho(\omega, \theta)$ for fixed θ along the variable ξ . In other words, when keeping θ fixed in the Fourier domain, this slice of the Fourier Transform of $\bar{\mu}(\omega, \theta)$ corresponds exactly to the 1-D Fourier Transform of the Radon Transform for that θ , *i.e.*, $\rho_{\theta}(\xi)$. This is the **central slice theorem**. Alternatively, replacing each column of the sinogram by its Fourier Transform gives the Fourier Transform of μ in polar coordinates.

Need some figures

1.6 Filtered Backprojection

The central slice theorem allows us to recover $\mu(x, y)$ from the measurements using the inverse Fourier Transform and a change of coordinates from the

Cartesian coordinates (ω_x, ω_y) to the polar coordinates ω, θ .

$$\begin{aligned}
\mu(x, y) &= \frac{1}{4\pi^2} \int_{-\infty}^{\infty} \int_{-\infty}^{\infty} \bar{\mu}(\omega_x, \omega_y) e^{i\omega_x x} e^{i\omega_y y} d\omega_x d\omega_y \\
&= \frac{1}{4\pi^2} \int_0^\pi \int_{-\infty}^{\infty} \bar{\mu}(\omega, \theta) e^{i\omega(\cos\theta)x} e^{i\omega(\sin\theta)y} |\omega| d\omega d\theta \\
&= \frac{1}{2\pi} \int_0^\pi \left[\frac{1}{2\pi} \int_{-\infty}^{\infty} \bar{\mu}(\omega, \theta) |\omega| e^{i\omega(x \cos\theta + y \sin\theta)} d\omega \right] d\theta. \quad (14)
\end{aligned}$$

The inner integral in the square brackets is the one-dimensional inverse Fourier Transform of $\bar{\mu}(\omega, \theta)|\omega|$ along the variable ω with fixed θ . Define

$$\rho^*(\xi, \theta) = \mathcal{F}^{-1}[\bar{\mu}(\omega, \theta)|\omega|] = \frac{1}{2\pi} \int_{-\infty}^{\infty} \bar{\mu}(\omega, \theta) |\omega| e^{i\omega(x \cos\theta + y \sin\theta)} d\omega. \quad (15)$$

Then

$$\mu(x, y) = \frac{1}{2\pi} \int_0^\pi \rho_\theta^*(x \cos\theta + y \sin\theta) d\theta. \quad (16)$$

Equation (16) provided the recipe for recovery of μ :

- 1) *Filtering step*: From $\rho(\xi, \theta)$, find $\rho^*(\xi, \theta) = \mathcal{F}_\omega^{-1}\{\mathcal{F}_\xi\{\rho(\xi, \theta)\}|\omega|\}$,
- 2) *Backprojection*: Sum over $\rho^*(\xi, \theta)$ over all θ .

The first step is called the filtering step because it seems to be interpretable as a convolution: Observing that a product in the Fourier domain is a convolution in the spatial domain it is tempting to write

$$\rho^*(\xi, \theta) = \rho(\xi, \theta) * \mathcal{F}^{-1}\{|\omega|\}. \quad (17)$$

However, the function $|\omega|$ has infinite energy and such a split into two functions is not valid. A different split is possible:

$$\mathcal{F}_\omega^{-1}\{\mathcal{F}_\xi\{\rho(\xi, \theta)\}|\omega|\} = \mathcal{F}_\omega^{-1}\left\{\frac{\mathcal{F}_\xi\{\rho(\xi, \theta)\}}{H(w)} \cdot H(w)|\omega|\right\} \quad (18)$$

$$= \mathcal{F}_\omega^{-1}\left\{\frac{\mathcal{F}_\xi\{\rho(\xi, \theta)\}}{H(w)}\right\} * \mathcal{F}_\omega^{-1}\{H(w)|\omega|\}, \quad (19)$$

where $H(\omega)$ is expected to decrease sufficiently fast to compensate for the increase by $|\omega|$ so that $\mathcal{F}_\omega^{-1}\{H(w)|\omega|\}$ exists. If $\rho(\xi, \theta)$ is band-limited so that frequencies beyond Ω are not present,

$$\mathcal{F}_\xi\{\rho(\xi, \theta)\} = 0 \text{ when } \omega > \Omega, \quad (20)$$

then we can design $H(\omega)$ to be 1 up to Ω , and then drop monotonically to zero.

$$\begin{cases} H(\omega) = 1, & |\omega| \leq \Omega \\ H(\omega) \neq 0, & \text{otherwise.} \end{cases} \quad (21)$$

In this case we have we have

$$\mathcal{F}_\omega^{-1}\left\{\frac{\mathcal{F}_\xi\{\rho(\xi, \theta)\}}{H(\omega)}\right\} = \mathcal{F}_\omega^{-1}\left\{\frac{\mathcal{F}_\xi\{\rho(\xi, \theta)\}}{1}\right\} = \rho(\xi, \theta), \quad (22)$$

and

$$\rho^*(\xi, \theta) = \rho(\xi, \theta) * \mathcal{F}_\omega^{-1}\{H(\omega)|\omega|\}. \quad (23)$$

The filter $H(\omega)$ can be designed a number of ways. First, the filter defined by Ramachandran and Lakshiminarayanan [23], known now as the *Ram-Lak* filter, is simply obtained by limiting the frequency domain response, Figure(5).

$$H(\omega) = \begin{cases} 1, & |\omega| \leq \Omega \\ 0, & \text{otherwise.} \end{cases} \quad (24)$$

so that the overall filter is $H_{RL}(\omega) = H_{RL}(\omega)|\omega|$, or,

$$H_{RL}(\omega) = \begin{cases} |\omega|, & |\omega| \leq \Omega \\ 0, & \text{otherwise.} \end{cases} \quad (25)$$

Using Appendix(C), Formula 3, the spatial domain filter is

$$h_{RL}(x) = \frac{\Omega^2}{\pi} \left[\text{sinc}(\Omega x) - \frac{1}{2} \text{sinc}^2\left(\frac{\Omega x}{2}\right) \right], \quad (26)$$

See Figure(5).

Second, the *Shepp-Logan* filter [25] has a similar design that it also limits the frequency upper bound, but in contrast to the Ram-Lak filter, it does so gradually using a *sinc* function $\frac{2\Omega}{\pi} \text{sinc}\left(\frac{\pi\omega}{2\Omega}\right)$, Figure(5), with the overall filter defined as

$$H_{SL}(\omega) = \begin{cases} \left| \sin\left(\frac{\pi\omega}{2\Omega}\right) \right|, & |\omega| < \Omega \\ 0, & \text{otherwise} \end{cases} \quad (27)$$

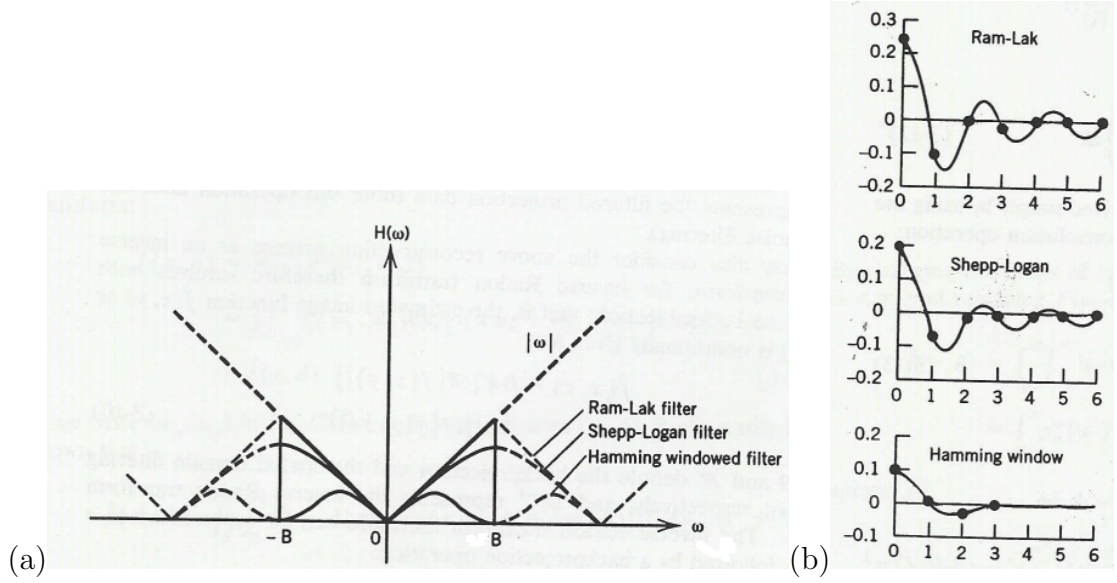


Figure 5: (a) Examples of the band-limited filter function of sampled data. Note the cyclic repetitiveness of the digital filter. (b) Spatial domain filter kernels corresponding to the filter functions shown in the Ram-Lak filter is a high-pass filter with a sharp response but results in some noise enhancement, while the Shepp-Logan and the Hamming window filters are noise-smoothed filters and therefore have better SNR. (Images taken from [3])

The spatial filter corresponding to the Shepp-Logan filter is

$$\begin{aligned}
 h_{SL}(\omega) &= \frac{1}{2\pi} \int_{-\infty}^{\infty} H_{SL}(\omega) e^{i\omega x} d\omega \\
 &= \frac{1}{2\pi} \int_{-\Omega}^{\Omega} \left| \sin\left(\frac{\pi\omega}{2\Omega}\right) \right| e^{i\omega x} d\omega \\
 &= \frac{1}{2\pi} \int_0^{\Omega} 2 \sin\left(\frac{\pi\omega}{2\Omega}\right) \cos \omega x d\omega \\
 &= \frac{1}{2\pi} \int_0^{\Omega} \sin\left(\left(\frac{\pi}{2\Omega} + x\right)\omega\right) d\omega + \frac{1}{2\pi} \int_0^{\Omega} \sin\left(\left(\frac{\pi}{2\Omega} - x\right)\omega\right) d\omega \\
 &= \frac{-1}{2\pi} \frac{\cos\left(\left(\frac{\pi}{2\Omega} + x\right)\omega\right)}{\left(\frac{\pi}{2\Omega} + x\right)} \Bigg|_0^{\Omega} - \frac{1}{2\pi} \frac{\cos\left(\left(\frac{\pi}{2\Omega} - x\right)\omega\right)}{\left(\frac{\pi}{2\Omega} - x\right)} \Bigg|_0^{\Omega} \\
 &= \frac{1}{2\pi} \frac{1 - \cos\left(\frac{\pi}{2} + \Omega x\right)}{\frac{\pi}{2\Omega} + x} + \frac{1}{2\pi} \frac{1 - \cos\left(\frac{\pi}{2} - \Omega x\right)}{\frac{\pi}{2\Omega} - x} \\
 &= \frac{1}{2\pi} \frac{1 + \sin(\Omega x)}{\frac{\pi}{2\Omega} + x} + \frac{1}{2\pi} \frac{1 - \sin(\Omega x)}{\frac{\pi}{2\Omega} - x} \\
 &= \frac{1}{2\pi} \frac{1}{\left(\frac{\pi}{2\Omega}\right)^2 - x^2} \left[\frac{\pi}{\Omega} - 2x \sin(\Omega x) \right] \\
 &= \frac{1}{\pi} \frac{\frac{\pi}{2\Omega} - x \sin(\Omega x)}{\left(\frac{\pi}{2\Omega}\right)^2 - x^2}.
 \end{aligned}$$

The Ram-Lak filter has the following formula in the spatial domain when sampled at Nyquist rate which is two times the bandwidth of a bandlimited signal so that $\Delta x = \frac{\pi}{\Omega}$:

$$H(k) = \begin{cases} \frac{\pi}{4}, & \text{if } k=0 \\ -\frac{1}{\pi k^2}, & \text{if } k \text{ odd} \\ 0, & \text{if even} \end{cases}$$

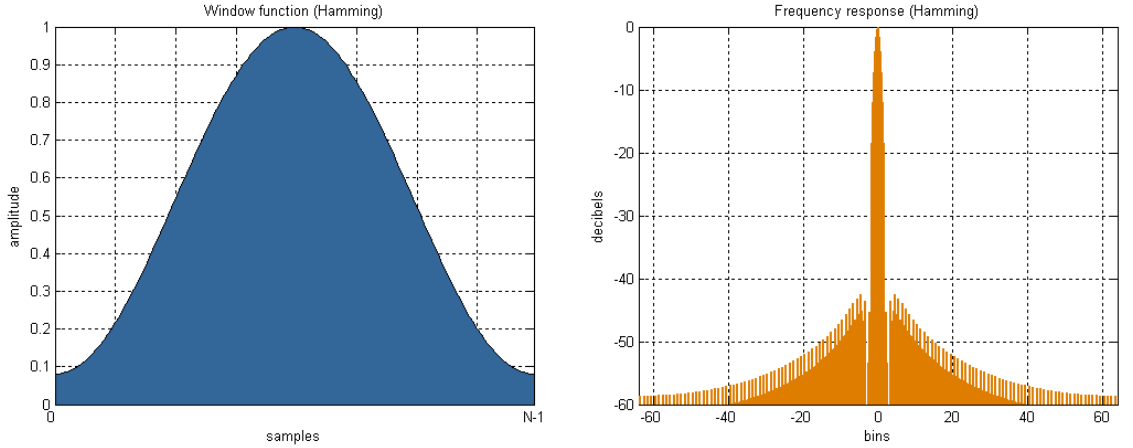
while the Shepp-Logan filter is given by:

$$H(k) = \frac{-8\Omega^2}{\pi^2(4k^2 - 1)}, \quad k = 0, \pm 1, \pm 2, \dots$$

in the spatial domain.

Explain the Hamming Window approach proposed originally by Richard Hamming. using the raised cosine:

$$w[n] = 0.54 - 0.46 \cos\left(\frac{2\pi n}{N-1}\right). \quad (28)$$



In a different approach, Rosenfeld and Kak [24] use $H(\omega) = e^{-\epsilon|\omega|}$ so that the overall filter is $H_\epsilon(\omega) = |\omega|e^{-\epsilon|\omega|}$. In the spatial domain this filter is written as $h_\epsilon(x) = \frac{\epsilon^2 - (2\pi x)^2}{[\epsilon^2 + (2\pi x)^2]^2}$. This filter is plotted in Figure(6) for several values of ϵ .

It is not clear why a filter that balances being 1 in the range up to Omega and smaller after that has not been used:

$$H_{Kim} = \frac{|\omega|}{1 + \left(\frac{\omega}{\Omega}\right)^6}. \quad (29)$$

Note: Add a formal definition of backprojection as “Adjoint Radon Transform.”

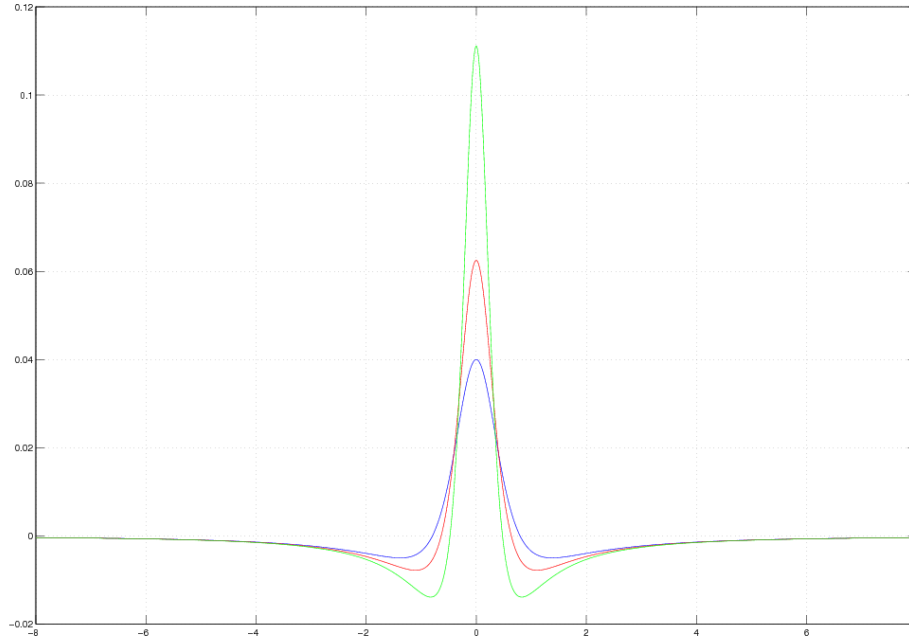


Figure 6: The approximate reconstruction filter $h_\epsilon(x)$ from [24] plotted for $\epsilon = 5$ (blue), $\epsilon = 4$ (red) and $\epsilon = 3$ (green).

1.7 Watch out for those singularities: A review of Calculus

What do you do when the integrand has a singularity? Consider the integral

$$I = \int_{-a}^a \frac{1}{\sqrt{x}} dx, \quad (30)$$

where the integrand blows up at $x = 0$; what happens to the value of the integral? A substitution $y = \sqrt{x}$ gives

$$I = \frac{1}{2} \int_{-\sqrt{a}}^{\sqrt{a}} dy = \sqrt{a}, \quad (31)$$

a finite value, even when $a \rightarrow 0$. Now consider the integral

$$II = \int_{-a}^a \frac{1}{x^2} dx. \quad (32)$$